Pixel detectors for particle physics and imaging applications ☆

N. Wermes*

Physikalisches Institut der Universität Bonn, Nussallee 12, Bonn 53115, Germany

Abstract

Semiconductor pixel detectors offer features for the detection of radiation which are interesting for particle physics detectors as well as for imaging e.g., in biomedical applications (radiography, autoradiography, protein crystallography) or in X-ray astronomy. At the present time hybrid pixel detectors are technologically mastered to a large extent and large-scale particle detectors are being built. Although the physical requirements are often quite different, imaging applications are emerging and interesting prototype results are available. Monolithic detectors, however, offer interesting features for both fields in future applications. The state of development of hybrid and monolithic pixel detectors, excluding CCDs, and their different suitability for particle detection and imaging, is reviewed.
© 2003 Elsevier B.V. All rights reserved.

PACS: 07.77.Ka; 85.30; 85.40.−e; 87.59.−e; 87.59.Bh; 07.85.Fv

Keywords: Pixeldetector; Semiconductor detector

1. Introduction

The requirements on semiconductor pixel detectors for charge particle detectors in high energy physics compared to those from imaging can be very different. In particle physics experiments individual charged particles, usually triggered by other subdetectors, have to be identified with high demands on spatial resolution and timing. In imaging applications the image is obtained by the un-triggered accumulation (integrating or counting) of the quanta of the impinging radiation, often also with high demands (e.g., $\gtrsim 1$ MHz per pixel in certain radiography or CT applications). Si pixel detectors for high energy charge particle detection can assume typical signal charges collected at an electrode in the order of 5000–10,000 electrons even taking into account charge sharing between cells and detector deterioration after irradiation to doses as high as 60 Mrad. In tritium autoradiography, on the contrary, or in X-ray astronomy the amount of charge to be collected with high efficiency can be much below 1000e. The spatial resolution is governed by the attainable pixel granularity from a few to about 10 μm at best, obtained with pixel dimensions in the order of 50–100 μm. The requirements from radiology (mammography) are similar, while some applications in autoradiography require sub-μm resolutions, not attainable with present day pixel

detectors. For applications with lower demands on the spatial resolution ($\mathcal{O}(10\ \mu m)$) but with demands on real time and time resolved data acquisition, semiconductor pixel detectors are however attractive.

Thin detector assemblies are mandatory for the vertex detectors at collider experiments, in particular for the planned linear e^+e^- collider. While silicon is almost a perfect material for particle physics detectors, allowing the shaping of electric fields by tailored impurity doping, the need of high photon absorption efficiency in radiological applications requires the study and use of semiconductor materials with high atomic charge, such as GaAs or CdTe. For such materials the charge collection properties are much less understood and mechanical issues in particular those related to hybrid pixels are abundant, most notably regarding the hybridization of detectors when they are not available in wafer scale sizes. Last but not least the cost-performance ratio is an important factor to consider if an imaging application should be commercially interesting.

2. Hybrid pixel detectors for particle physics

In the "hybrid pixel technique" sensor and FE-chips are separate parts of the detector module connected by the small conducting bumps applied by using the bumping and flip-chip technology. All of the LHC-collider-detectors [1–3] ALICE, ATLAS, and CMS, LHCb for the RICH system [4], as well as some fixed target experiments (NA60 [5] at CERN and BTeV [6] at Fermilab) employ the hybrid pixel technique to build large-scale ($\sim m^2$) pixel detectors. Pixel area sizes are either rectangular (typically 50 μm $\times$ 400 μm as for ATLAS) or quadratic (150 μm $\times$ 150 μm as for CMS). The detectors are arranged in cylindrical barrels of 2–3 layers and disks covering the forward and backward regions. The main purpose that these detectors must serve is (a) identification of short lived particles (e.g., b-tagging for Higgs and SUSY signals), (b) pattern recognition and event reconstruction and (c) momentum measurement, in this order of importance. Among the technical issues of high demand which must be addressed the need to

withstand a total (10 years) particle fluence of $10^{15} n_{eq}$ corresponding to a radiation dose of about 60 Mrad is the most demanding one. The discovery that oxygenated silicon is radiation hard with respect to the nonionizing energy loss of protons and pions [7] saves pixel detectors at the LHC for which this radiation is most severe due to their proximity to the interaction point. n^+ electrode in n-bulk material sensors have been chosen to cope with the fact that type inversion occurs after about $2.5 \times 10^{13} n_{eq}$. After type inversion the pn-diode sits on the electrode side thus allowing the sensor to be operated partially depleted. Fig. 1(a) shows the layout of the ATLAS pixel sensor [8]. The n^+ pixels are isolated against each other by the moderated p-spray technique [8,9]. The bias grid at the bottom allows to test the sensor before bonding to the electronics ICs is made. All pixels are set under voltage by the punch through biasing mechanism. Fig. 1(b) shows the charge collected in two adjacent pixels after irradiation with 2×10^{15} protons/cm^2, the full LHC dose after 10 years. A tolerable loss in charge collection efficiency is observed at the punch-through point, which goes at the expense of the biasing feature which is too important to be sacrificed, and at the edge of the pixel. Everywhere else the collection even after this high dose is homogeneous. The sensors can be operated after irradiation with bias voltages in excess of 600 V in full depletion. Pixel sensors for the LHC detectors are close to or already in production in large quantities.

The requirements on the FE-chip also impose severe constraints on noise, threshold dispersion, timewalk and power consumption. After several chip generations first in radiation soft CMOS and BiCMOS technologies and later in the radiation hard DMILL and $\frac{1}{4}$ micron technologies have at last produced FE-ICs with the required performance and decent yield in excess of 60%. After irradiation to the full LHC dose, the ATLAS $\frac{1}{4}$ micron pixel chip FE-I shows noise values of about 250e and threshold dispersions in the range of $\sim$70e after threshold tuning. The power consumption per pixel is about 50 μW.

The process of chip and sensor connection called hybridization is done by fine pitch bumping
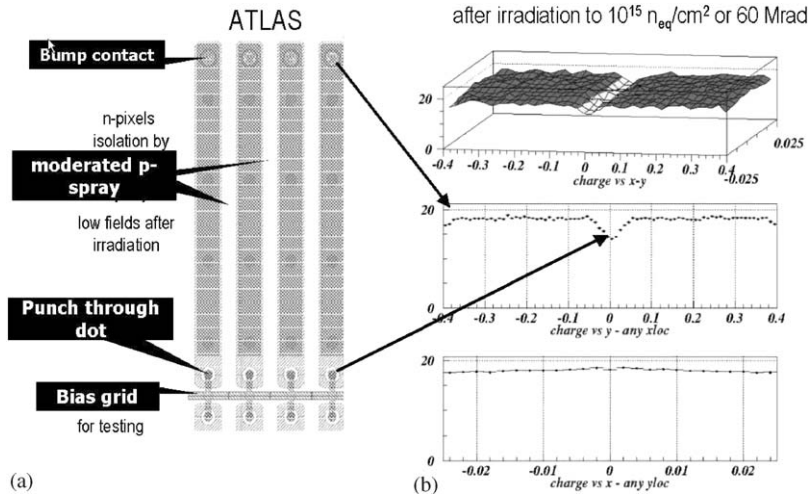
Fig. 1. (a) Layout of the ATLAS pixel sensor, (b) results of charge collection measurements obtained in testbeam running with detectors and chips which were irradiated to 60 Mrad.
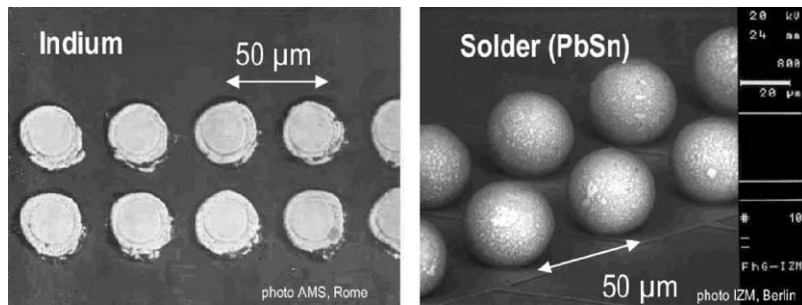

Fig. 2. (left) Indium (Photo AMS, Rome) and (right) solder (PbSn, Photo IZM, Berlin) bump rows with 50 μm pitch.

and subsequent flip-chip which is achieved with either PbSn (solder) or indium bumps at a failure rate of $< 10^{-4}$. Fig. 2 shows rows of 50 μm pitch bumps obtained by these techniques.

Indium bumps are applied using a wet lift-off technique applied on both sides (sensor and IC) [10]. The connection is obtained by thermo-compression. The Indium joint is comparatively soft and the gap between IC and sensor is about 6 μm. PbSn bumps are applied by electroplating [11]. Here the bump is galvanically grown on the chip wafer only. The bump is connected by flip-chipping to an under-bump metallization to the sensor substrate pixel. Both technologies have

been successfully used with 8'' IC-wafers and 4'' sensor wafers.

In the case of ATLAS sixteen FE-chips are bump connected to a silicon sensor to form a *module* of 2.1×6.4 cm^2 area (Fig. 3(a)). The I/O lines of the chips are connected via wire bonds to a kapton flex circuit glued atop the sensor. The flex houses a module control chip (MCC) responsible for front end time/trigger control and event building. The total thickness at normal incidence is in excess of 2% of a radiation length.

The modules are arranged in ladders (staves) and cooled by evaporation of a fluorinert liquid (C_4F_{10} or C_3F_8) at an input temperature below
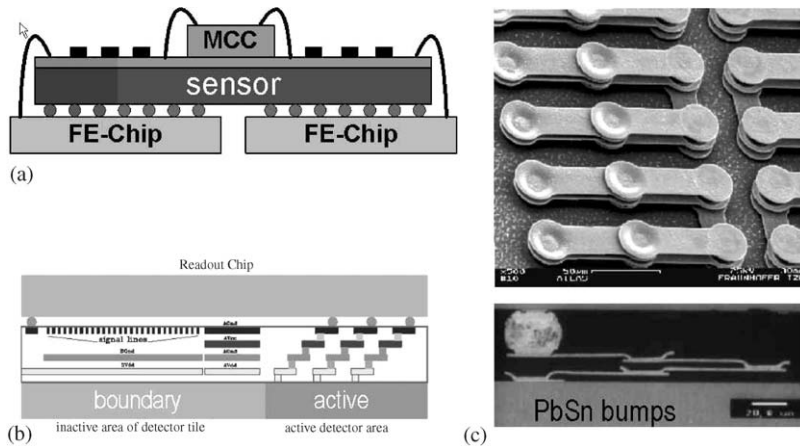
Fig. 3. (a) Schematic view of a hybrid pixel module showing ICs bonded via bump connection to the sensor, the flex hybrid kapton layer atop the sensor with mounted electrical components, and the module control chip (MCC). Wire bond connections are needed as indicated. (b) Schematic layout of an MCM-D pixel module. (c) SEM photograph of an MCM-D via structure (top) and a cross-section after bump deposition (bottom).

−20°C in order to maintain the entire detector below −6°C to minimize the damage induced by radiation. This operation requires pumping and the cooling tubes must stand 8 bar pressure if pipe blocking occurs. All detector components must withstand temperature cycles between −25°C and room temperature.

In summary, the Hybrid Pixel Technology is *the* present-day technology for large area pixel detectors in particle physics. Several pixel vertex detectors are in production for LHC and other experiments. Some potentially major issues still exist, most notably yield issues which in this technology come into play in many areas as chip-wafer and sensor-wafer yields, bumping and flip-chipping yields, as well as burn-in yields of modules with 16 ICs and about 50,000 individual amplifier channels.

What are the possible future advances and directions and what are the limitations of the hybrid pixel technology? The area of a pixel cell is limited by the readout circuitry obtainable for a given area. With the availability of chip technologies with small structure sizes ($\leqslant 0.25\,\mu$m) the target pixel size can be made substantially smaller than planned for the first generation of large area hybrid pixel detectors. Area sizes of $\sim 50 \times 50\,\mu$m^2 or somewhat below are, however, at the

limit for this technology in my opinion. The limit for small pitch bumping is in the order of 10–20 μm [12]. An interesting alternative to the flex-kapton solution to provide power and signal distribution to and from the module is the so-called multi-chip-module technology deposited on Si-substrate (MCM-D), pioneered by IZM (Berlin), for pixel particle detectors in collaboration with Wuppertal University [13]. A multi-conductor-layer structure is built up on the silicon sensor. This allows to bury all bus structures in four layers in the inactive area of the module thus avoiding the kapton flex layer and any wire bonding at the expense of a small thickness increase of 0.1% X_0. Fig. 3(b) illustrates the principle and Fig. 3(c) shows scanning electron microphotographs (ref. IZM, Berlin) of a via structure made in MCM-D technology.

3. Hybrid pixel detectors for imaging applications

3.1. Radiology

There is a vast amount of radiology detection and imaging techniques. The discussion in this paper will be limited to an application which possibly opens new directions in radiology due to

fully digital imaging, i.e., pixel detectors with individual X-ray photon counting in every pixel cell. This approach offers many features which are very attractive for X-ray imaging: excellent linearity and an infinite dynamic range (at least in principle), optimal exposure times and a good image contrast compared to conventional film-foil-based radiography thus avoiding over- and under-exposed images. There are very interesting developments using integrating methods such as flat panel imagers based on a-Si [14] or a-Se technologies [15], which are to be considered the state of the art in large area radiography. Their review, however, is beyond the scope of this paper and is referred to dedicated conferences (see, for instance, Ref. [16]).

Two counting hybrid pixel detector developments are called MEDIPIX [17], a CERN-based collaboration and MPEC [18] at Bonn University. The challenges to be addressed in order to become competitive with integrating systems are: high speed ($\gtrsim 1$ MHz) counting with at least 15 bit, operation with very little dead time, low noise and particularly low threshold operation with small threshold dispersion values. In particular the last item is important in order to allow homogeneous imaging of soft X-rays. It is also mandatory for a differential energy measurement, realized so far as a double threshold with energy windowing logic [19,20]. A differential measurement of the energy, exploiting the different shapes of X-ray spectra behind for example tissue or bone, can enhance the contrast performance of an image. The idea of using a linear feedback shift register as a small counter which fits in a pixel area was first realized in Ref. [21] and is implemented in both, MPEC and MEDIPIX, circuits. Finally, for radiography high photon absorption efficiency is mandatory, which renders the not easy task of high Z sensors and their hybridization necessary.

The MEDIPIX chip (version 2) [20] uses 256×256, $55\,\mu m \times 55\,\mu m$ large pixels fabricated in $0.25\,\mu m$ technology, energy windowing via two tunable discriminator thresholds, and a 15 bit counter. The maximum count rate per pixel is about 1 MHz. Fig. 4 shows an X-ray scan of a sardine taken in successive scanning steps with the MEDIPIX1 chip (64×64 pixels,
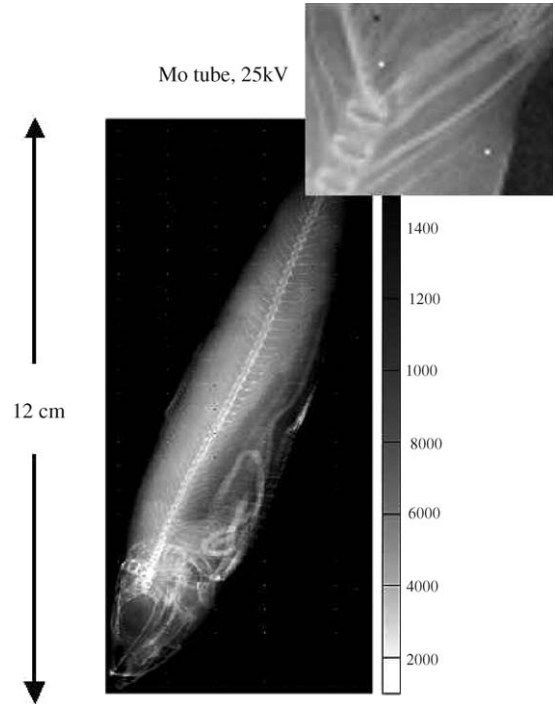

Fig. 4. Image of a sardine obtained with the MEDIPIX1 counting pixel chip with Si sensor obtained by successive scans.

$170\,\mu m \times 170\,\mu m$) using an Si sensor. GaAs sensors have also been successfully operated.

Imaging sensor systems [22,23] using the MPEC chip have been made also with high Z semiconductors for more efficient X-ray absorption. A technical issue here is the bumping of individual die sensors of Cd(Zn)Te or GaAs. This has been solved at ISAS, Tokyo in collaboration with Mitsubishi Industries and Bonn University by employing double Au-stud bumps with In-filling material in order to account for thickness inhomogeneities in the sensor surface [23]. Fig. 5 shows an image of a nut and that of a screw obtained with a CdTe sensor using the MPEC2.3 counting chip. The MPEC chip features 32×32 pixels ($200\,\mu m \times 200\,\mu m$), double threshold operation, 18-bit counting at ~ 1 MHz per pixel as well as low noise values ($\sim 120e$ with CdTe sensor) and threshold dispersion (21e after tuning).

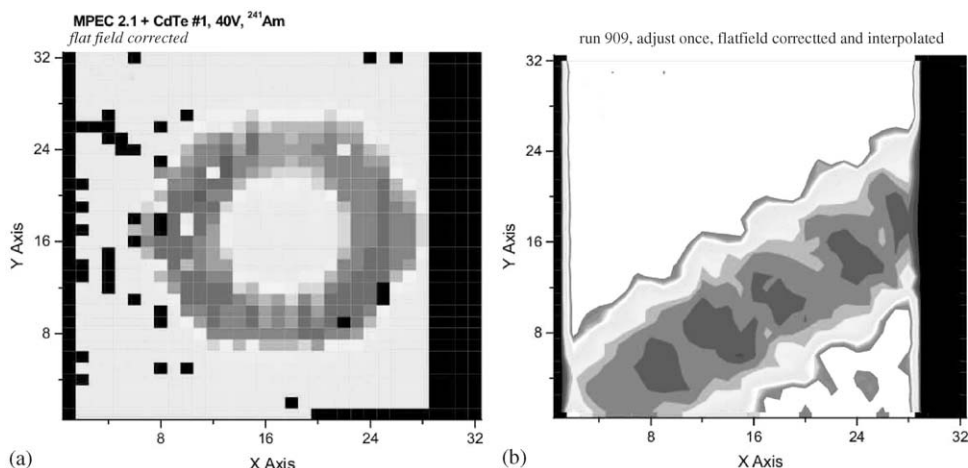Both MPEC and MEDIPIX developments now address modules with a larger detection area

Fig. 5. X-ray (^{241}Am) images, obtained with the MPEC chip (32×32 pixels, 200 μm $\times$ 200 μm) and a CdTe sensor, of a nut (a) and a screw in (b). The screw profile indicates the good contrast quality obtainable by digital X-ray imaging employing single photon counting.

($5–10$ cm^2) and high-Z sensors. While the counting pixel approach is new and interesting for imaging applications, it will be difficult to compete on a short time scale with already commercially available integrating systems such as flat panel imagers [14,15]. The possible market value of photon counting pixel systems is not yet explored.

3.2. Crystallography

Counting hybrid pixel detectors are also starting to become used in protein crystallography with synchrotron radiation. Here the challenge is to image Bragg patterns produced by scattered X-ray photons of typically 6 keV or higher at a high rate (typ. $1–1.5$ MHz/pixel). The typical spot size of a diffraction maximum is $100–200$ μm, calling for pixel sizes in the order of $100–300$ μm. The high linearity of the hit counting method and the absence of so-called "blooming effects", i.e., the response of nonhit pixels in the close neighborhood of a Bragg maximum, makes these detectors very appealing for protein crystallography experiments. Developments are underway for ESRF (Grenoble, France) and SLS (Swiss Light Source at the Paul-Scherrer Institute, Switzerland) beam lines. The XPAD detector

[24] (330 μm $\times$ 330 μm pixels) planned for ESRF beam lines has modules with 10 chips bonded to a 4×1.6 cm^2 silicon substrate. The PILATUS detector [25] at the SLS (217 μm $\times$ 217 μm pixels) is made of sixty 16 chip modules each covering 8×3.5 cm^2, i.e., a total area of 40×40 cm^2. The maximum count rate of both detectors is $1–1.5$ MHz/pixel. A delicate threshold tuning question remains to obtain a homogenous response function of the detectors also at the pixel boundaries where a loss of charge on a pixel occurs due to charge sharing and may lead to hit losses. Fig. 6 shows a diffraction image of Ag-Behenate obtained with the XPAD detector [26].

In conclusion, the hybrid pixel technique has been established also for imaging using silicon and high-Z material such as GaAs or CdTe. The method of photon counting in every pixel offers at least in principle the possibility of an infinite dynamic range and linearity, giving hope for a new quality of experiments with synchrotron light detectors. For radiology the use of double (multiple) thresholds is interesting to enhance the contrast performance. It will, however, be very demanding to go much beyond a count rate of about 1 MHz per pixel and to produce large area detectors.
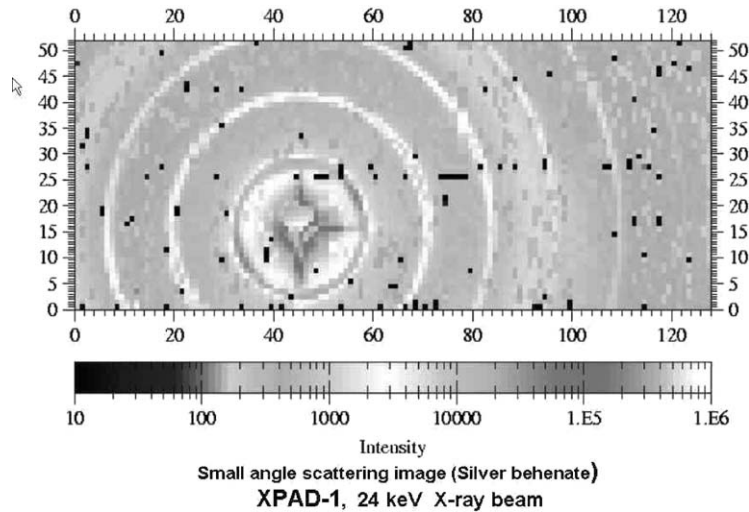
Fig. 6. Bragg diffraction pattern obtained with the XPAD hybrid counting pixel detector [24].

4. Monolithic pixel detectors

Monolithic pixel detectors, in which amplifying and logic circuitry as well as the radiation detecting sensor are made from one piece of silicon, have been the dream of semiconductor detector physicists. The first monolithic pixel detector, successfully operated in a particle beam was made by Snoeys and collaborators [27] as early as in 1992. They used a high purity, high resistivity p-type bulk pin-diode in which the junction has been created by an n-type diffusion layer. On one side, an array of ohmic contacts to the substrate served as collection electrodes. An array of 10×30 pixels with $125\,\mu m \times 34\,\mu m$ pixel cells has been realized and successfully operated in a particle beam. However, no large-scale detector evolved from this development.

A new era calling for monolithic pixel or CCD vertex detectors is that of future colliders most notably linear e^+e^- colliders, where very low ($\ll 1\% X_0$) material per layer, small pixel sizes ($\sim 20\,\mu m \times 20\,\mu m$) and very high rate capability (80 hits/mm²/ms) is required. This is due to the very intense beam strahlung of narrowly focussed electron beams close to the interaction region which produces electron positron pairs in vast numbers. High readout speeds of 50 MHz with 40 µs frame time are required. These challenges are addressed at the TESLA collider [28] by CMOS CCDs [29], CMOS Active Pixel Sensors [30] and DEPFET pixel detectors [31,38].

4.1. CMOS active pixels

CMOS active pixel detectors as they are used in CMOS cameras are suited also for the detection of minimum ionizing particles. However, their fill factor is much less than 100% and the total chip area is small. MIMOSA[1] active pixel sensors (MAPS) [30] have been developed to overcome these deficiencies. As shown in Fig. 7 the epitaxial layer of a standard CMOS (0.6 or 0.35 µm) process is used for the generation of electron–hole pairs. They are trapped between potential barriers on both sides of the epi-layer and reach, by thermal diffusion, an n-well/p-epi collection diode, rendering small pixel sizes a necessity and not a demand. The sensor is depleted only directly under this n-well diode. Only here full charge collection is obtained. Matrix operation is done using a standard 3-transistor readout commonly employed by CMOS matrix devices (see Fig. 8(a)). A line of the matrix is selected by transistor M3, the signal is
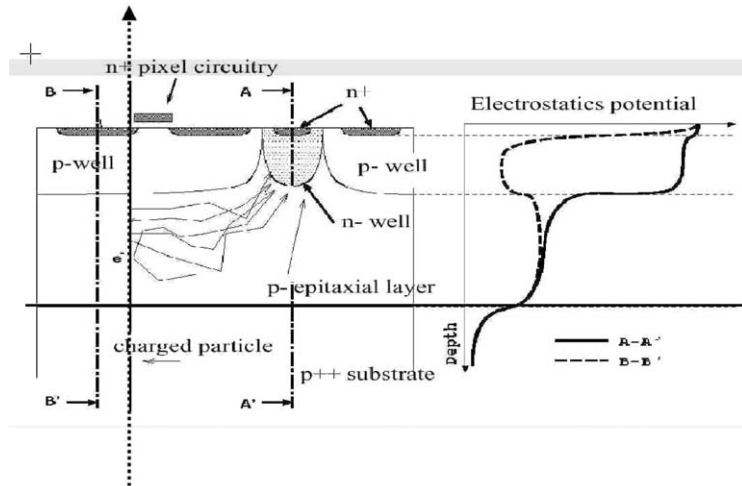
---

[1] Minimum ionizing MOS array.

Fig. 7. Cross-section and potential profile of the MAPS. Charge created in the epitaxial layer reaches the n-well collecting diode by diffusion.
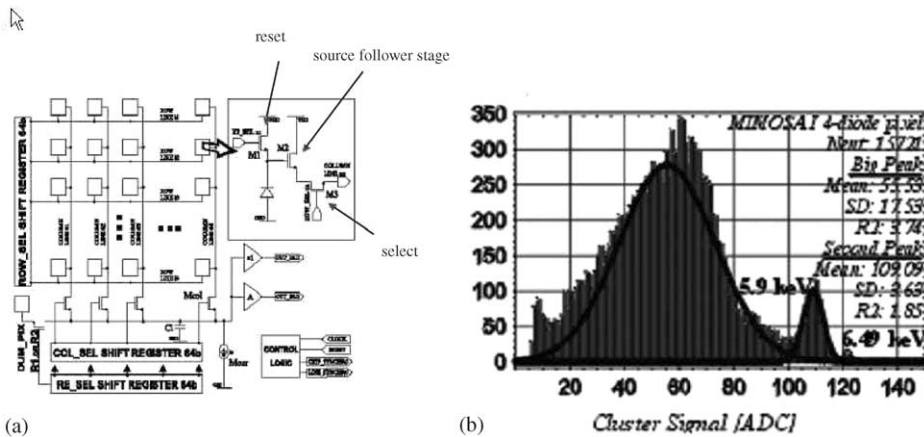

Fig. 8. (a) Matrix operation of MAPS-monolithic pixels. (b) Response to an [55]Fe5.9 keV X-ray source. An interpretation is given in the text.

readout via a source follower stage (M2), and reset by transistor M1. The charge obtained for a signal from a high energy particle is in the order of only 1000e or less, the collection time is ∼100 ns, but low noise values (15–30e) and small pixel sizes (20 μm × 20 μm) can be achieved. This is demonstrated in Fig. 8(b) which shows the response to an [55]Fe 5.9 keV X-ray signal. The small peak corresponds to hits entering in the small depleted region under the n-well. The large peak is due to X-rays absorbed in the undepleted area of a pixel.

Summarizing PROs and CONs of CMOS monolithic pixel detectors for particle physics I would conclude that from the above-mentioned 'dream' of fully monolithic CMOS charge sensing, amplification, readout and logic, one is still a bit away. While the low cost (potentially ∼1$ for 4096 pixels) for 'off-the-shelf' CMOS sensors is indeed a very attractive feature, a 100% area fill factor still requires a special development and R&D programe (like MIMOSA APS). In the active area, due to the n-well collection diode, no CMOS (only NMOS) circuitry is possible. The

voltage signals are very small ($\sim$mV), of the same order as transistor threshold dispersions which at least requires some dedicated design effort. At present [32] also a severe radiation tolerance issue exists. While the MAPS sensors withstand nonionizing radiation (neutrons) up to about 10^{12}–10^{13} n/cm^2, ionizing radiation, even soft X-rays, impose a serious problem for present designs as the devices stop functioning already after $\sim$200 krad. This is under investigation. It seems that the radiation sensitivity is not inherently due to the MAPS sensor structure itself. Last, but not least, the necessity of a sufficiently thick epitaxial layer as charge collection layer, renders only a few processing technologies suited for sensors. With the rapid change of commercial process technologies this also is an issue of concern. The CMOS camera market may save these developments.

4.2. DEPFET pixels

The Depletion Field Effect Transistor (DEP-FET) pixel principle [33] has been and is being developed for three very different application areas: particle physics vertex detection [31], X-ray astronomy [34,35], and biomedical autoradiography [36]. Fig. 9 shows the principle of operation of this device. On a sidewards depleted bulk (Si) the potential for electrons is formed such that the minimum is located about 1 μm below the top surface. By additionally shaping the potentials of bulk, source and drain of an implanted JFET or MOS transistor on the pixel's surface, aided by a deep-n implantation under the gate region, a local potential minimum for electrons is formed under the transistor channel which acts as an 'internal gate'. The holes created by the impinging radiation drift towards the rear contact, the electrons are collected and stored in the potential bucket of the internal gate, thereby changing its potential resulting in a modulation of the channel current of the implanted transistor. The collected electrons are removed from the internal gate by a clear pulse applied to a dedicated contact outside the transistor region or by other clear mechanisms e.g., through the external gate by punch-through to the internal gate.

The very low input capacitance and the in situ amplification (i.e., charge to current conversion) of the device makes DEPFET pixel detectors very attractive for low noise operation. The latter is very important for low energy X-ray astronomy and for autoradiography applications. For particle physics, where the signal charge is large in comparison, this feature can be used to design very thin detectors [31,37] ($\sim$30 μm) with very low power consumption when operated as a rowwise selected matrix. Depending on the application, i.e., for very low noise operation in spectroscopy or very fast readout in particle physics the device is operated in source follower readout mode or drain current readout mode (see paper given at this conference [38]). Fig. 10 shows the response of a single DEPFET pixel operated in source follower readout mode to an ^{55}Fe source. The measured energy resolution is

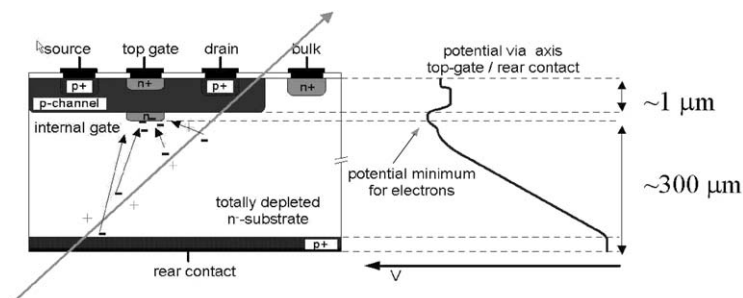$$\Delta E = 130 \text{ eV} \quad @ \ 6 \text{ keV}$$

Fig. 9. Principle of operation of a DEPFET pixel structure. Cross-sectional view (left) of a half-pixel with symmetry axis at the left edge, and potential profile (right).
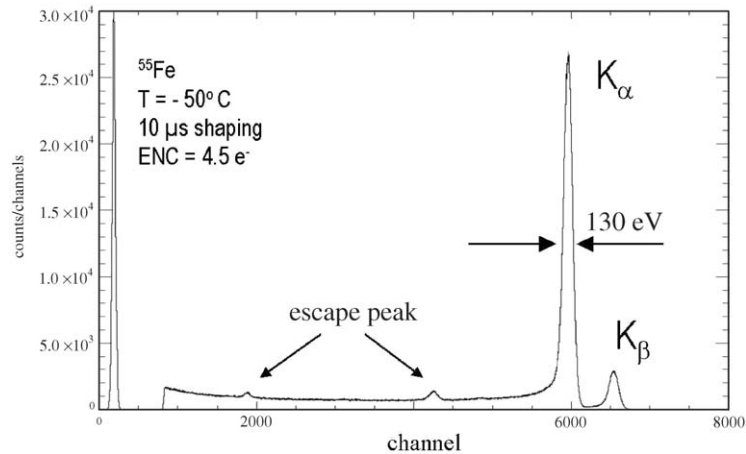
Fig. 10. Response of a DEPFET pixel detector to an ^{55}Fe X-ray source (Mn K$_\alpha$5984 eV, Mn K$_\beta$ eV)obtained using a single pixel device operated at -50°C with a shaping time of 10 μs.
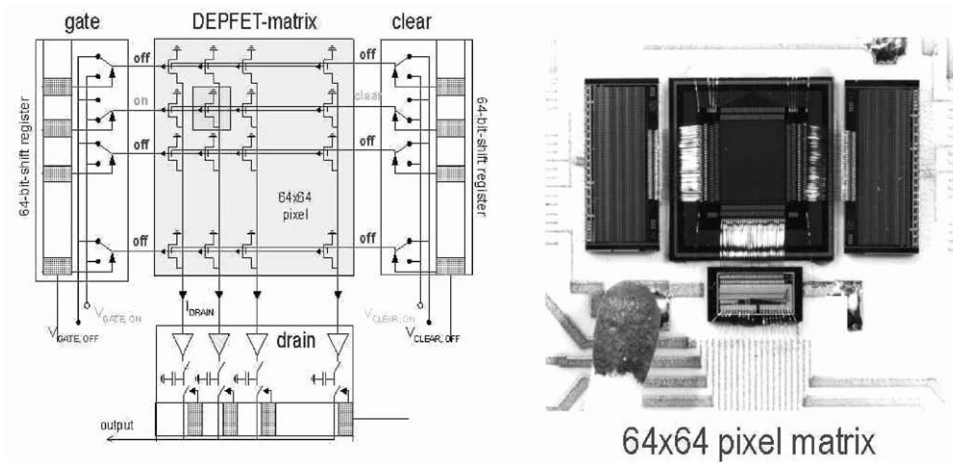

Fig. 11. Principle of operation (left) and photograph (right) of a DEPFET pixel matrix showing two steering ICs for gate and clear control, respectively, as well as the current amplification stage at the bottom.

at a temperature of -50°C. Very similar values were also obtained at room temperature. The noise contribution is dominated by Fano noise ($\sim$14e at 6 keV and RT). The DEPFET structure itself contributes with 4.5e, mostly $1/f$, channel noise.

Fig. 11 shows the principle of operation of a large pixel matrix [39]. Rows are selected by applying a voltage to the external gate of a row. Drains are connected columnwise. The drain current of each pixel in a selected row is detected and amplified in a dedicated amplification circuit. Pedestals are taken the same way several cycles

before and subtracted. Finally, clear pulses are applied to the clear contacts to empty the internal gates.

In imaging operation spatial resolutions of

27 lp/mm   @ 30%MTF

have been measured [36].

DEPFET pixel matrices are presently being developed for low noise high energy resolution operation in the X-ray satellite project XEUS [34] and for high speed, high spatial resolution in the TESLA vertex detector [31]. A DEPFET Bioscope
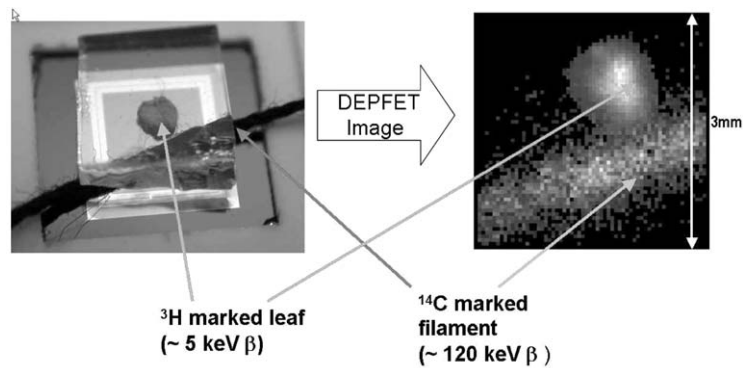
Fig. 12. Autoradiography image of bio-material radio-labelled with two different radio-markers (^{3}H and ^{14}C) obtained with a DEPFET pixel detector.

matrix has already been used [39] in autoradiographical imaging of tritium marked biological samples. Fig. 12 demonstrates the successful separation of two different radio markers (^{3}H and ^{14}C) with high spatial resolution [40].

5. Summary

Driven by the demands for high spatial resolution, high rate particle detection in high energy physics, semiconductor pixel detectors have also started to become exploited for imaging applications. Hybrid pixel detectors, in which sensor and electronic chip are separate entities, connected via bump bonding techniques represent today's state of the art for both, particle detection and imaging applications. Monolithic detectors, in the form of CMOS sensors, are already used for imaging in CMOS cameras. For the detection of high energy particles they are so far of limited use mainly because their fill factor is much smaller than 1, i.e., less than 100% detection coverage, and their radiation tolerance is weak. The next generation of collider experiments, however, will have to target monolithic pixel detectors. Present approaches in this direction are: MAPS which try to overcome the limitations of CMOS camera chips, and pn-DEPFET Pixel Detectors which are also very attractive for (low energy) X-ray astronomy and autoradiographical imaging.

References

[1] Technical Design Report of the ATLAS Pixel Detector, CERN/LHCC/98-13 (1998).
[2] CMS, the Tracker System Project, Technical Design Report, CERN/LHCC/98-006 (1998);
W. Erdmann, The CMS pixel detector, Nucl. Instr. and Meth. A 447 (2000) 178–183.
[3] ALICE Technical Design Report, CERN/LHCC 99-12 (1999);
F. Antinori, A pixel detector system for ALICE, Nucl. Instr. and Meth. A 395 (1997) 404–409.
[4] T. Gys, The pixel hybrid photon detectors for the LHCb-RICH project, Nucl. Instr. and Meth. A 465 (2001) 240–246.
[5] A. Baldit, et al., CERN-SPSC-2000-010 (2000);
C. Lourenco, E. Radermacher, CERN-SPSC-2002-025 (2002).
[6] BTeV Proposal (2000), FNAL document http://www-btev.fnal.gov/DocDB/0000/000066/002/index.html.
[7] ROSE Collaboration, G. Lindström, et al., Nucl. Instr. and Meth. A 466 (2001) 308–326;
G. Lindström, Paper Presented at this Conference (9th European Symposium on Semiconductor Detectors, Elmau, 2002); Nucl. Instr. and Meth. A, these Proceedings.
[8] M.S. Alam, et al., Nucl. Instr. and Meth. A 456 (2001) 217–232.
[9] R. Richter, Paper Presented at this Conference (9th European Symposium on Semiconductor Detectors, Elmau, 2002).

[10] C. Gemme, Study of indium bumping for the ATLAS pixel detector, Nucl. Instr. and Meth. A 465 (2001) 200–203.

[11] G. Engelmann, J. Wolf, L. Dietrich, S. Fehlberg, O. Ehrmann, H. Reichl, Proceedings of the 1999 Joint International Meeting of the Electrochemical Society, Hawaii, Vol. 99(2), 1999, p. 907;
J. Wolf, PbSn60 Solder Bumping by Electroplating, Pixel2000 Workshop, Genova, Italy, June 2000.

[12] O. Ehrmann, Fraunhofer Institut IZM, Berlin, private communication.

[13] P. Gerlach, C. Linder, K.H. Becks, Nucl. Instr. and Meth. A 473 (2001) 102–106 and references therein;
M. Töpper, International Conference on High Density Packaging and MCMs, Denver, Colorado, April 1999.

[14] T. Ducourant, et al., Proc. SPIE 3977 (2000) 14–25;
N. Jung, et al., Proc. SPIE 3336 (1998) 396–407.

[15] O. Tousignant, et al., Proc. SPIE 4682 (2002) 503–510.

[16] Proceedings of the SPIE Conference on Medical Imaging, San Diego, 2002.

[17] M. Campbell, E.H.M. Heijne, G. Meddeler, E. Pernigotti, W. Snoeys, IEEE Trans. Nucl. Sci. NS-45 (3) (1998) 751–753;
Medipix Collaboration, S.R. Amendiola, et al., Nucl. Instr. and Meth. A 422 (1999) 201–205;
Medipix Collaboration, S.R. Amendiola, et al., Nucl. Instr. and Meth. A 466 (2001) 74–78.

[18] P. Fischer, J. Hausmann, M. Overdick, B. Raith, N. Wermes, L. Blanquart, V. Bonzom, P. Delpierre, Nucl. Instr. and Meth. A 405 (1998) 53–59;
P. Fischer, et al., IEEE Trans. Nucl. Sci. NS-46 (4) (1999) 1070;
L. Blanquart, V. Bonzon, G. Comes, P. Delpierre, P. Fischer, J. Hausmann, M. Keil, M. Lindner, S. Meuser, N. Wermes, Nucl. Instr. and Meth. A 439 (2000) 80–90.

[19] P. Fischer, A. Helmich, M. Lindner, N. Wermes, L. Blanquart, IEEE Trans. Nucl. Sci. NS-47 (3) (2000) 881–884;
M. Lindner, L. Blanquart, P. Fischer, H. Krüger, N. Wermes, Nucl. Instr. and Meth. A 465 (2000) 229–234.

[20] X. Llopart, M. Campbell, R. Dinapoli, D. SanSegundo, E. Pernigotti, Proceedings of the NSS/MIC Conference, San Diego, 2001, IEEE Trans. Nucl. Sci. NS-49 (2002) 2279.

[21] P. Fischer, An area efficient 128 channel counter chip, Nucl. Instr. and Meth. A 378 (1996) 297–300.

[22] M. Lindner, et al., Nucl. Instr. and Meth. A 466 (2000) 63–73;
M. Lindner, et al., Nucl. Instr. and Meth. A 466 (2000) 63.

[23] P. Fischer, M. Kouda, H. Krüger, M. Lindner, G. Sato, T. Takahashi, S. Watanabe, N. Wermes, preprint, IEEE Trans. Nucl. Sci. (2001), submitted for publication;
P. Fischer, M. Kouda, S. Krimmel, H. Krüger, M. Lindner, M. Löcker, G. Sato, T. Takahashi, S. Watanabe, N. Wermes, Single Photon X-Ray Imaging with Si- and CdTe-Sensors, International Workshop on Radiation Imaging Detectors, Orosei, Sardinien, September 2001, Nucl. Instr. and Meth. A, submitted for publication.

[24] P. Delpierre, J.F. Berar, L. Blanquart, B. Caillot, J.C. Clemens, C. Mouget, IEEE Trans. Nucl. Sci. NS-48 (4) (2001) 987–991;
P. Delpierre, J.F. Berar, L. Blanquart, N. Boudet, P. Breugnon, B. Caillot, J.C. Clemens, I. Koudobine, C. Mouget, R. Potheau, I. Valin, NSS-MIC/IEEE, San Diego (USA), November 4–10, 2001, IEEE Trans. Nucl. Sci. NS-49 (2002) 902; 2518.

[25] C. Brönnimann, et al., J. Syn. Rad. 7 (2000) 301.

[26] P. Delpierre (CPPM, Marseille), private communication.

[27] W. Snoeys, et al., IEEE Trans. Nucl. Sci. NS-39 (1992) 1263.

[28] TESLA Technical Design Report, DESY-01-011 (2001).

[29] T. Behnke, S. Bertolucci, R.D. Heuer, R. Settles, TESLA Technical Design Report, Part 4, DESY-01-011 (2001).

[30] R. Turchetta, et al., Nucl. Instr. and Meth. A 458 (2001) 677–689;
M. Deveaux, G. Deptuch, Ninth European Symposium on Semiconductor Detectors, Elmau, 2002; Nucl. Instr. and Meth. A, these Proceedings.

[31] P. Fischer, M. Schumacher, M. Trimpl, J. Ulrici, N. Wermes, L. Andricek, G. Lutz, R. Richter, Desy Linear Collider Note LC-DET-2002-004 (2002).

[32] W. Dulinski (Strasbourg), private communication.

[33] J. Kemmer, G. Lutz, Nucl. Instr. and Meth. A 253 (1987) 356.

[34] P. Holl, P. Fischer, P. Klein, G. Lutz, W. Neeser, L. Strüder, N. Wermes, Active Pixel Matrix for X-ray Satellite Missions, IEEE Trans. Nucl. Sci. NS-47 (4) (2000) 1421;
L. Strüder, et al., Proc. SPIE 4012 (2000) 200–217.

[35] P. Lechner, paper submitted to this conference, in: Ninth European Symposium on Semiconductor Detectors, Elmau, 2002.

[36] W. Neeser, et al., IEEE Trans. Nucl. Sci. NS-47 (3) (2000) 1246;
P. Klein, et al., Nucl. Instr. and Meth. A 454 (2000) 152–157.

[37] L. Andricek, MPI-Munich, private communication.

[38] P. Fischer, Readout Concepts for DEPFET Pixel Detectors, Ninth European Symposium on Semiconductor Detectors, Elmau, 2002; Nucl. Instr. and Meth. A, these Proceedings.

[39] J. Ulrici, S. Adler, P. Buchholz, P. Fischer, P. Klein, M. Löcker, G. Lutz, W. Neeser, L. Strüder, M. Trimpl, N. Wermes, Nucl. Instr. and Meth. A 465 (2001) 247–252.

[40] J. Ulrici (Bonn Univ.), private communication.